Journal of Mechanical Research and Application JMRA
ISSN: 2251-7383, eISSN: 2251-7391
Vol. 4, No. 1, 2012, 53-63

Vibration of Cracked Plate Using Differential Quadrature Method and Experimental Modal Analysis

S. Moradi [1*], P. Alimouri [2]

Received: 17 July 2012; Accepted: 16 August 2012

Abstract: In this study, the vibration of cracked plates is investigated using differential quadrature method and experimental modal analysis. The crack, which is assumed to be open, is modeled by the extended rotational spring. With its finite length, the crack divides the plate into six segments. Then, the differential quadrature is applied to the governing differential equations of motion and the corresponding boundary and continuity conditions. An eigenvalue analysis is performed on the resulting system of algebraic equations to obtain the natural frequencies of the cracked plate. To ensure the integrity and robustness of the presented method, experimental modal analysis is carried out on cantilever plates having open cracks with finite length and the results are compared with the proposed method. A numerical study is performed to show the effect of length, depth and location of the crack on natural frequencies of the plates. The results verify the accuracy and efficiency of differential quadrature method.

Keywords: Differential Quadrature Method, Cracked Plate, Experimental Modal Analysis

1. Introduction

Plates are one of the mostly used structures in different industries. Crack in a structure results in reduction in local stiffness and therefore reduces its strength. Any changes in the stiffness of structure affect the modal parameters such as natural frequencies and mode shapes. Therefore, it can be a starting point in detection of faults in structures. The basic idea behind the vibration based inspection methods is that the damage in the structures can be identified and characterized based on the changes in dynamic properties like natural frequencies, mode shapes and damping. Parabhakara and Datta [1] investigated the stability and vibration of plates having local defects. They modeled the defect with reduction in elastic properties in its location and used the finite element method to solve the problem.

Khadem and Rezaee [2] introduced modified comparative functions to analyze the vibration of simply supported rectangular cracked plates. They considered the elastic behavior of the plate at crack location as a line spring with a varying stiffness along the crack. Liew et al. [3] investigated the vibrating behavior of cracked rectangular plates using domain decomposition method. They assumed the plate to be an assemblage of small sub-domains with the appropriate shape functions, and derived a governing eigenvalue equation that could be solved to obtain the vibration frequencies of cracked plate. Ismail and Cartmell [4] utilized an analytical approach to study the forced vibrations of a plate having a crack of variable angular orientation. Xing and Liu [5] used the method of separation of variables to obtain the closed form solutions for the free vibrations of rectangular Mindlin plates. Fan and Qiao [6] applied 2-D continuous wavelet transform on the mode shape of composite plate structures for damage detection. They confirmed their approach by an experimental modal test on some impacted composite plates.

Natarajan et al. [7] investigated the linear free bending vibrations of functionally graded material plates with a through- center crack using a shear flexible finite element. Hu and Wu [8] developed a scanning damage index based on the ratio of modal

1*. Corresponding Author: Associate Professor, Department of Mechanical Engineering, Shahid Chamran University, Ahvaz, Iran (moradis@scu.ac.ir)
2. M.Sc., Department of Mechanical Engineering., Shahid Chamran University, Ahvaz, Iran (alimouri_p@yahoo.com)

strain energy of the structure before and after damage to identify the surface crack in a plate structure. In order to compute the modal strain energy they used the differential quadrature method. By performing tests on an aluminum alloy thin plate with a surface crack, they validated their proposed method. Hosseini-Hashemi et al. [9] proposed a set of exact closed form characteristic equations to study the vibration behavior of moderately thick rectangular plates having arbitrary number of all-over part-through cracks with continuously distributed line-spring model. Shahban and Alipour [10] analyzed the free vibration of functionally graded thick circular plates resting on elastic foundation with elasticity restrained edges using the differential transformation method. Huang et al. [11, 12] solved the problem of free vibration of side-cracked rectangular thick plates made of isotropic and functionally graded materials using Ritz Method. They used special admissible functions to account for the stress singularity behavior around the crack.

In this study, the vibration analysis of plate structures having a finite length open crack is investigated utilizing the differential quadrature (DQ) method and experi-mental modal analysis. The results are compared with those of finite element analysis. Furthermore, several experimental case studies on cantilever plates having finite cracks are performed to demonstrate the accuracy of the proposed method.

2. Modeling of damaged plate

Fig. 1 shows a thin rectangular elastic cantilever plate of dimensions a and b, and thickness H, having a finite- length surface crack.

The crack position from the clamped side is l_c, and its length and depth are b_2 and h, respectively. The presence of the crack, which results in reduction in plate stiffness at its position, can be modeled by rotational spring. Therefore, the crack with finite length divides the plate into six segments as shown in Fig. 2.

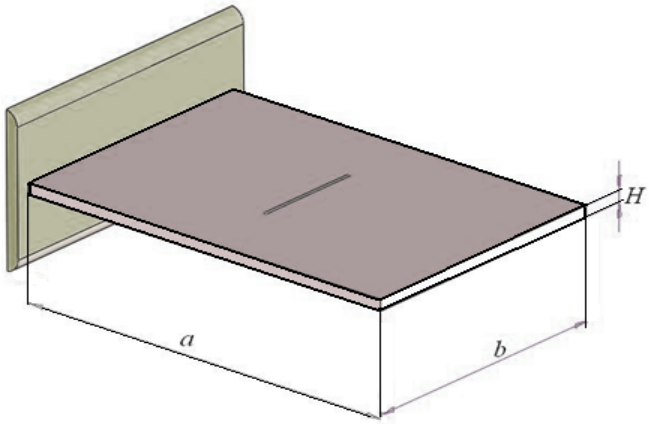

Fig. 1. Geometry of cracked cantilever plate.

The differential equation of motion for the bending vibration of the segments can be described by the following Eq.(1) [13]:

$$\frac{\partial^4 w_q}{\partial x^4} + 2\frac{\partial^4 w_q}{\partial x^2 \partial y^2} + \frac{\partial^4 w_q}{\partial y^4} = \Omega^2 w_q; \quad q = 1,2,...,6 \tag{1}$$

Where w_q is the deflection of the segment q, and Ω is the dimensionless natural frequency of the plate which can be expressed by Eq. (2):

$$\Omega = \omega a^2 \sqrt{\frac{\rho H}{D}} \tag{2}$$

ω is the natural frequency of the plate, ρ is the density and D is the flexural rigidity of the plate defined by Eq. (3):

$$D = \frac{EH^3}{12(1-\upsilon^2)} \tag{3}$$

where E and υ being Young's modulus and Poisson's ratio of the plate material, respectively. The boundary conditions considered here are those of clamped and free edges, continuity conditions at the interfaces of segments, and discontinuity conditions due to the presence of the crack between regions 3 and 4. The deflection and rotation at clamped supports are set to be zero:

$$W_q = 0 \qquad \text{at } x = 0 \qquad q = 1,3,5 \tag{4-a}$$

$$\frac{\partial W_q}{\partial x} = 0$$

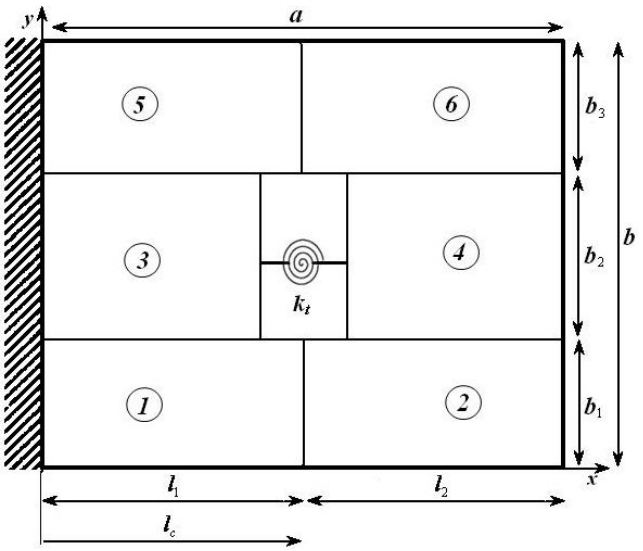

Fig. 2. Sub sectioning of plate domain.

The plate experiences neither bending moments nor shear forces at the free edges in x direction:

$$\frac{\partial^2 W_q}{\partial x^2}+\nu\frac{\partial^2 W_q}{\partial y^2}=0$$

$$q=2,4,6 \qquad \text{(4-b)}$$

$$\frac{\partial^3 W_q}{\partial x^3}+(2-\nu)\frac{\partial^3 W_q}{\partial y^2\partial x}=0$$

and in y direction:

$$\frac{\partial^2 W_q}{\partial y^2}+\nu\frac{\partial^2 W_q}{\partial x^2}=0$$

$$q=1,2,5,6 \qquad \text{(4-c)}$$

$$\frac{\partial^3 W_q}{\partial y^3}+(2-\nu)\frac{\partial^3 W_q}{\partial x^2\partial y}=0$$

Besides, the boundary conditions at the free corners are:

$$\frac{\partial^2 W_q}{\partial x\partial x}=0 \qquad q=2,6 \qquad \text{(4-d)}$$

At the interfaces of regions 1 and 2, and 5 and 6, the deflections, rotations, bending moments and shear forces must be continuous in x direction:

$$W_q=W_l$$

$$\frac{\partial W_q}{\partial x}=\frac{\partial W_l}{\partial x} \qquad (q,l)=\begin{pmatrix}1,2\\5,6\end{pmatrix} \qquad \text{(4-e)}$$

$$\frac{\partial^2 W_q}{\partial x^2}+\nu\frac{\partial^2 W_q}{\partial y}=\frac{\partial^2 W_l}{\partial x^2}+\nu\frac{\partial^2 W_l}{\partial y^2}$$

$$\frac{\partial^3 W_q}{\partial x^3}+(2-\nu)\frac{\partial^3 W_q}{\partial x\partial y^2}=\frac{\partial^3 W_l}{\partial x^3}+(2-\nu)\frac{\partial^3 W_l}{\partial x\partial y^2}$$

At the interfaces of regions 1 and 3, 2 and 4, 3 and 5, and 4 and 6, the deflections, rotations, bending moments and shear forces must be continuous in y direction:

$$W_q=W_l$$

$$\frac{\partial W_q}{\partial y}=\frac{\partial W_l}{\partial y} \qquad (q,l)=\begin{pmatrix}1,3\\2,4\\3,5\\4,6\end{pmatrix} \qquad \text{(4-f)}$$

$$\frac{\partial^2 W_q}{\partial y^2}+\nu\frac{\partial^2 W_q}{\partial x^2}=\frac{\partial^2 W_l}{\partial y^2}+\nu\frac{\partial^2 W_l}{\partial x^2}$$

$$\frac{\partial^3 W_q}{\partial y^3}+(2-\nu)\frac{\partial^3 W_q}{\partial y\partial x^2}=\frac{\partial^3 W_l}{\partial y^3}+(2-\nu)\frac{\partial^3 W_l}{\partial y\partial x^2}$$

On the cracked sides, the boundary conditions consist of continuity of deflection, bending moment and shear force, and the discontinuity of slope due to the bending. The slope difference between the two sides of the plate at the crack front has been defined by Khadem and Rezaee [2] by Eq. (5):

$$\theta=-6H\left(\frac{\partial^2 W}{\partial x^2}+\nu\frac{\partial^2 W}{\partial y^2}\right)\alpha_{bb} \qquad (5)$$

where α_{bb} is the non-dimensional bending compliance defined by the following relation for any crack depth Eq. (6):

$$\alpha_{bb}=\frac{1}{H}\int_0^h g_b^2\,dh \qquad (6)$$

g_b is a dimensionless function of the crack depth to plate thickness ratio ($\xi=h/H$) defined by Gross [14] as Eq. (7):

$$g_b=\xi^{\frac{1}{2}}(1.99-247\xi+1297\xi^2-23.117\xi^3+24.80\xi^4); \qquad 0<\xi<0.7 \qquad (7)$$

Therefore, the boundary condition over the cracked edge can be expressed by the following expressions:

$$\begin{aligned}
&W_3 = W_4\\
&\frac{\partial W_3}{\partial x} - \theta = \frac{\partial W_4}{\partial x}\\
&\frac{\partial^2 W_3}{\partial x^2} + \nu\frac{\partial^2 W_3}{\partial y^2} = \frac{\partial^2 W_4}{\partial x^2} + \nu\frac{\partial^2 W_4}{\partial y^2}\\
&\frac{\partial^3 W_3}{\partial x^3} + (2-\nu)\frac{\partial^3 W_3}{\partial x \partial y^2} = \frac{\partial^3 W_4}{\partial x^3} + (2-\nu)\frac{\partial^3 W_4}{\partial x \partial y^2}
\end{aligned} \tag{8}$$

Applying the DQ to Eq. (1) results in the following equation:

$$\begin{aligned}
&\sum_{m=1}^{N_x} C_{imq}^{(4)} W_{mjq} + 2\phi^2 \sum_{m=1}^{N_x}\sum_{n=1}^{N_y} C_{imq}^{(2)} B_{jnq}^{(2)} W_{mnq}\\
&\quad + \phi^4 \sum_{n=1}^{N_y} B_{jnq}^{(4)} W_{mnq} = \Omega^2 W_{ijq}; q = 1,2,...,6
\end{aligned} \tag{9}$$

where $C_{ijq}^{(k)}$ and $B_{ijq}^{(k)}$ are the weighting coefficients of the *k*th-order partial derivative of the *q*th region with respect to x and y, respectively. Here the domain is divided into N_x discrete points in the *x*-direction and N_y in *y*-direction. W_{ij} is the deflection of the grid point laying on the intersection of the *i*th point in *x*-direction and *j*th point in *y*-direction. ϕ is the plate aspect ratio (i.e. $\phi = a/b$).

The clamped boundary conditions in Eq. (4a) are transformed into the following format (Eq. 10-a):

$$W_{1jq} = 0; \frac{1}{l_q}\sum_{m=1}^{N_x} C_{1mq}^{(1)} W_{mjq} = 0; \quad \begin{matrix} q = 1,3,4 \\ i = 1,...,N_y \end{matrix} \tag{10-a}$$

The boundary conditions correspond to the free edges in *x* direction can be expressed in differential quadrature form by:

$$\begin{aligned}
&\sum_{m=1}^{N_x} C_{N_x m}^{(2)} W_{mjq} + \nu\phi_q^2 \sum_{n=1}^{N_y} B_{jn}^{(2)} W_{N_x nq} = 0 \;;\; q = 2,4,6\\
&\sum_{m=1}^{N_x} C_{N_x m}^{(3)} W_{mjq} + (2-\nu)\phi_q^2 \sum_{m=1}^{N_x}\sum_{n=1}^{N_y} C_{N_x m}^{(1)} B_{jn}^{(2)} W_{mnq} = 0
\end{aligned} \tag{10-b}$$

and in *y* directions are Eqs. (10-a) and (10-d):

$$\begin{aligned}
&\phi_q^2 \sum_{n=1}^{N_y} B_{1n}^{(2)} W_{inq} + \nu\sum_{m=1}^{N_x} C_{im}^{(2)} W_{m1q} = 0 \;;\; q = 1,2\\
&\phi_q^2 \sum_{n=1}^{N_y} B_{1n}^{(3)} W_{inq} + (2-\nu)\sum_{m=1}^{N_x}\sum_{n=1}^{N_y} C_{im}^{(2)} B_{1n}^{(1)} W_{mnq} = 0
\end{aligned} \tag{10-c}$$

$$\begin{aligned}
&\phi_q^2 \sum_{n=1}^{N_y} B_{N_y n}^{(2)} W_{inq} + \nu\sum_{m=1}^{N_x} C_{im}^{(2)} W_{mN_y q} = 0 \;;\; q = 5,6\\
&\phi_q^2 \sum_{n=1}^{N_y} B_{N_y n}^{(3)} W_{inq} + (2-\nu)\sum_{m=1}^{N_x}\sum_{n=1}^{N_y} C_{im}^{(2)} B_{N_y n}^{(1)} W_{mnq} = 0
\end{aligned} \tag{10-d}$$

where ϕ_q is the aspect ratio of the *q*th region. The differential quadrature representation of the free corners can be expressed as Eq. (10-e):

$$\phi_2 \sum_{m=1}^{N_x}\sum_{n=1}^{N_y} C_{N_x m}^{(1)} B_{1n}^{(1)} W_{mn2} = 0 \;;\; \phi_6 \sum_{m=1}^{N_x}\sum_{n=1}^{N_y} C_{N_x m}^{(1)} B_{N_y n}^{(1)} W_{mn6} = 0 \tag{10-e}$$

The continuity conditions of Eqs. (4-e) and (4-f) at the interfaces of the regions can be written as:

$$\begin{aligned}
&W_{N_x jq} = W_{1jl} \qquad (q,l) = \begin{pmatrix} 1,2 \\ 5,6 \end{pmatrix}\\
&\sum_{m=1}^{N_x} C_{N_x m}^{(1)} W_{mjq} = \beta \sum_{m=1}^{N_x} C_{1m}^{(1)} W_{mjl}\\
&\sum_{m=1}^{N_x} C_{N_x m}^{(2)} W_{mjq} + \nu\phi_q^2 \sum_{n=1}^{N_y} B_{jn}^{(2)} W_{N_x nq}\\
&\quad = \beta^2 \sum_{m=1}^{N_x} C_{1m}^{(2)} W_{mjl} + \nu\phi_q^2 \sum_{n=1}^{N_y} B_{jn}^{(2)} W_{1nl}\\
&\sum_{m=1}^{N_x} C_{N_x m}^{(3)} W_{mjq} + (2-\nu)\phi_q^2 \sum_{m=1}^{N_x}\sum_{n=1}^{N_y} C_{N_x m}^{(1)} B_{jn}^{(2)} W_{mnq}\\
&= \beta^3 \sum_{m=1}^{N_x} C_{1m}^{(3)} W_{mjl} + (2-\nu)\beta\phi_q^2 \sum_{m=1}^{N_x}\sum_{n=1}^{N_y} C_{1m}^{(1)} B_{jn}^{(2)} W_{mnl}
\end{aligned} \tag{10-f}$$

and

$$\begin{aligned}
&W_{iN_y q} = W_{i1l}\\
&\phi_q \sum_{n=1}^{N_y} B_{N_y n}^{(1)} W_{inq} = \phi_l \sum_{n=1}^{N_y} B_{1n}^{(1)} W_{inl} \qquad (q,l) = \begin{pmatrix} 1,3 \\ 2,4 \\ 3,5 \\ 4,6 \end{pmatrix}\\
&\phi_q^2 \sum_{n=1}^{N_y} B_{N_y n}^{(2)} W_{inq} + \nu\sum_{m=1}^{N_x} C_{im}^{(2)} W_{mN_y q} = \phi_l^2 \sum_{n=1}^{N_y} B_{1n}^{(2)} W_{inl} + \nu\sum_{m=1}^{N_x} C_{im}^{(2)} W_{m1l}\\
&\phi_q^3 \sum_{n=1}^{N_y} B_{N_y n}^{(3)} W_{inq} + (2-\nu)\phi_q \sum_{m=1}^{N_x}\sum_{n=1}^{N_y} C_{im}^{(2)} B_{N_y n}^{(1)} W_{mnq}\\
&\quad = \phi_l^3 \sum_{n=1}^{N_y} B_{1n}^{(3)} W_{inl} + (2-\nu)\phi_l \sum_{m=1}^{N_x}\sum_{n=1}^{N_y} C_{im}^{(2)} B_{1n}^{(1)} W_{mnl}
\end{aligned} \tag{10-g}$$

where $\beta=l_1/l_2$. At the cracked sides, the boundary conditions transform into the following equations:

$$
\begin{aligned}
&W_{Nj3} = W_{1j4}\\
&\sum_{m=1}^{N} C_{Nm}^{(1)} W_{nj3} - \theta = \beta \sum_{m=1}^{N} C_{1m}^{(1)} W_{nj4}\\
&\sum_{m=1}^{N} C_{Nm}^{(2)} W_{nj3} + \nu \phi_3^2 \sum_{n=1}^{N} B_{jn}^{(2)} W_{Nn3}\\
&= \beta^2 \sum_{m=1}^{N} C_{1m}^{(2)} W_{nj4} + \nu \phi_4^2 \sum_{n=1}^{N} B_{jn}^{(2)} W_{1n4}\\
&\sum_{m=1}^{N} C_{Nm}^{(3)} W_{nj3} + (2-\nu)\phi_3^2 \sum_{m=1}^{N}\sum_{n=1}^{N} C_{Nm}^{(1)} B_{jn}^{(2)} W_{nn3}\\
&= \beta^3 \sum_{m=1}^{N} C_{1m}^{(3)} W_{nj4} + (2-\nu)\beta\phi_3^2 \sum_{m=1}^{N}\sum_{n=1}^{N} C_{lm}^{(1)} B_{jn}^{(2)} W_{nn4}
\end{aligned}
\qquad \text{(10-h)}
$$

The combination of Eq. (9) and these boundary conditions can be represented by a system of linear equations, as Eq. (11):

$$
\begin{bmatrix} [A_{bb}] & [A_{bi}] \\ [A_{ib}] & [A_{ii}] \end{bmatrix} \begin{Bmatrix} W_b \\ W_i \end{Bmatrix} = \lambda \begin{bmatrix} 0 & 0 \\ B_{ib} & B_{ii} \end{bmatrix} \begin{Bmatrix} W_b \\ W_i \end{Bmatrix} \qquad (11)
$$

where the subscripts b and i denotes for the boundary and interior points used for writing the differential quadrature, respectively. The vector $\{W\}$ contains the deflections corresponding to the boundary and interior points. Transforming (11) into a general eigenvalue form in terms of $\{W_i\}$ results in Eq. (12).

$$
\left[A^*\right] \cdot \left\{W_i\right\} = \lambda \left[B^*\right] \cdot \left\{W_i\right\} \qquad (12)
$$

Solution of the above eigenvalue problem by a standard eigen solver, provides the natural frequencies of the cracked plate.

3. Experimental verification

In order to verify the integrity of differential quadrature method in real situations, an extensive experiment on cracked aluminum cantilever plates, was designed. The main purpose of the experiment is to comprehend the unavoidable measuring or modeling error which may contribute to the inaccuracy of natural frequencies obtaining with differential quadrature method. Mechanical properties of the test specimens such as density, Young's modulus and Poisson's ratio were measured experimentally, and are tabulated in Table 1 along with the plate dimensions.

First, the intact plates were tested. The excitation was carried out by a hammer (Global Test type AU02). A 1.5 gr. miniature accelerometer (B&K Type 4516) and a signal analyzer (B&K type 3032A) were utilized to measure the first three bending natural frequencies of the plate (see Fig. 3). In order to produce the clamped boundary condition, one should isolate the plate edge. In practice providing this condition needs a heavy fixture. Instead, to model clamped edge, one can use a distributed rotational spring at the plate edge. The rotational spring stiffness varies with the torque exerted on the fixture's bolts.

Table 1. Dimensions and mechanical properties of plate

υ	E (Gpa)	ρ (kg/m^3)	b (mm)	a (mm)	H (mm)
0.33	65.2	2652	100	200	2.85

Therefore, the stiffness should be evaluated for each plate separately, and no additional torque must be applied to the fixture throughout the tests. The first natural bending frequency of every intact plate was used to calculate the rotational spring stiffness. Then, the cracks with different depth and size were introduced in each plate at specified locations by using a special cutting tool. This ensures that the cracks remain open during the vibration. The generated cracks were in three relative locations (i.e. l_c/a=0.25, 0.5, 0.75), with three relative lengths (i.e. b_2/b=0.2, 0.5, 0.7) and three relative depths (i.e. ξ=0.2, 0.4, 0.6) of the plates. A total of 27 experiments were performed. At each step, the first three bending natural frequencies of the cracked plates were measured. The corresponding bending natural frequencies of the intact and cracked plates are presented in Table 2.

4. Results and Discussions

Several case studies were investigated to ensure the integrity and applicability of the proposed method. The effects of the relative crack depth, position and length on the natural frequencies of the plate represented by Fig. 3 were examined.

Table 2. Natural frequencies of cracked plate clamp edge

Case No.	l_c/a	b_2/b	h/H	Natural frequencies (Hz) ω^*_1	ω^*_2	ω^*_3
1	0.25	0.2	0.2	53.86	336.30	942.21
2			0.4	53.51	336.20	941.28
3			0.6	53.18	336.13	938.17
4		0.5	0.2	53.58	336.88	942.13
5			0.4	53.35	336.47	939.04
6			0.6	52.45	336.04	930.13
7		0.7	0.2	53.18	335.33	940.58
8			0.4	52.64	334.87	934.56
9			0.6	51.63	333.65	919.24
10		1	0.2	53.22	336.33	940.21
11			0.4	52.65	335.45	924.78
12			0.6	51.45	334.12	910.56
13	0.5	0.2	0.2	53.58	336.51	943.91
14			0.4	53.48	336.07	943.47
15			0.6	53.34	334.34	942.28
16		0.5	0.2	53.31	335.06	939.93
17			0.4	53.24	331.79	938.21
18			0.6	53.06	327.56	937.29
19		0.7	0.2	53.58	336.60	943.12
20			0.4	53.46	332.12	942.11
21			0.6	53.23	321.09	940.32
22		1	0.2	52.77	331.20	939.01
23			0.4	52.23	328.87	938.86
24			0.6	52.04	312.76	935.24
25	0.75	0.2	0.2	53.72	336.16	941.31
26			0.4	53.68	335.82	937.24
27			0.6	53.59	335.08	933.12
28		0.5	0.2	53.70	336.51	939.28
29			0.4	53.62	335.71	932.11
30			0.6	53.54	334.56	917.13
31		0.7	0.2	53.41	335.23	938.31
32			0.4	53.29	334.18	925.48
33			0.6	53.22	332.18	901.02
34		1	0.2	53.45	334.02	936.31
35			0.4	53.38	333.49	915.28
36			0.6	53.32	330.17	884.70

To assess the overall convergence efficiency of the DQ method, the first three experimental natural frequencies of the intact clamped plate (with the geometric and material properties of Table 1) are compared of the DQ and finite element methods. The finite element results are obtained using the ANSYS commercial software. The results are tabulated in Table 3. As can be seen from the table, the DQ results agree well with the experimental ones, and the errors are less than 0.4%. Moreover, the DQ results are in better agreement with the experiment compared with the result obtained from the finite element method.

The same comparison for the cracked plate is presented in Table 4. The plate used here has a crack with the relative length of 0.7 and relative depth of 0.6, located at the center of the plate. The

Table 3. Comparison between experimental and numerical frequencies of intact plate intact plate

	ω_1 (Hz)	Er (%)	ω_2 (Hz)	Er (%)	ω_3 (Hz)	Er (%)
Exper.	53.36	---	335.17	---	940.46	---
ANSYS	53.11	.84	337.30	.47	946.46	.64
DQ	53.76	.37	336.18	.14	942.38	.20

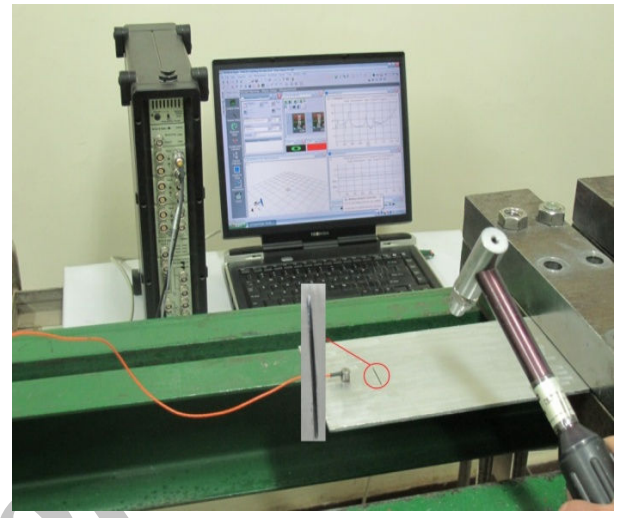

Fig. 3. General view of test equipment.

table shows that the DQ results agree well with those of experimental ones, and the maximum error is less than 0.6%.

Next, the effect of the crack depth on natural frequencies of clamped plate is investigated for different crack locations. The results are shown in Figs. 4-6.

It can be seen from the figures that increasing crack depth would result in a decrease in the natural frequencies of the plate. This is due to the fact that as the crack propagate through the depth of the plate, the bending compliance increases, resulting in the reduction of the plate stiffness and natural frequencies. Further-more, Fig. 5 shows that as the crack position reaches the free end, the change in natural frequency decreases and the crack loses its influence on the amount of dynamic parameters of the plate.

Table 4. Comparison between experimental and numerical frequencies of cracked plate

	ω_1 (Hz)	Er (%)	ω_2 (Hz)	Er (%)	ω_3 (Hz)	Er (%)
Exper.	53.23	---	321.09	---	940.32	---
ANSYS	52.68	1.33	322.79	0.53	945.86	0.59
DQ	53.51	0.53	322.18	0.34	942.21	0.19

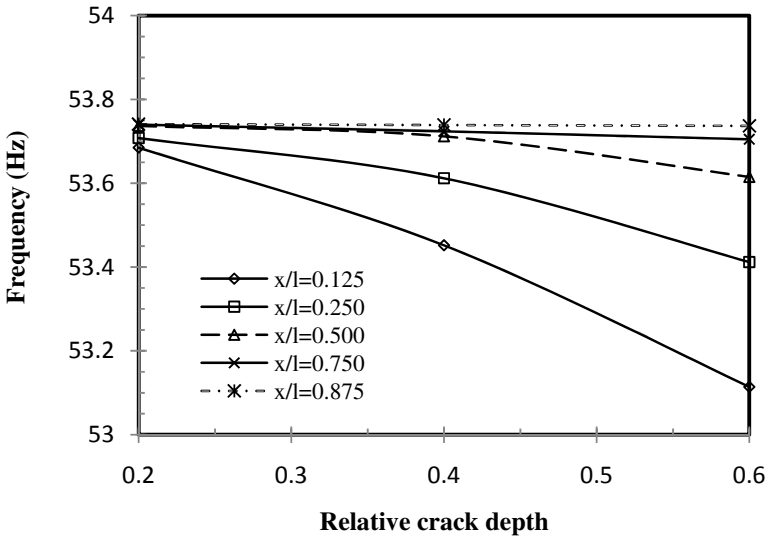

Fig. 4. Effect of relative crack depth on the 1st frequency.

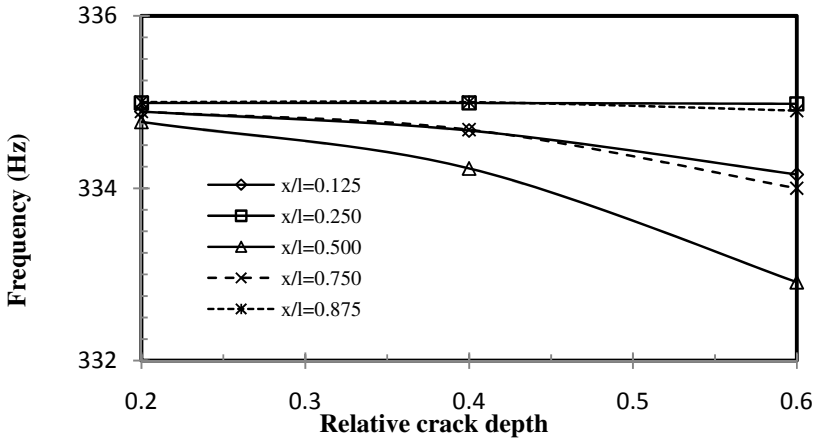

Fig .5. Effect of relative crack depth on the 2nd frequency.

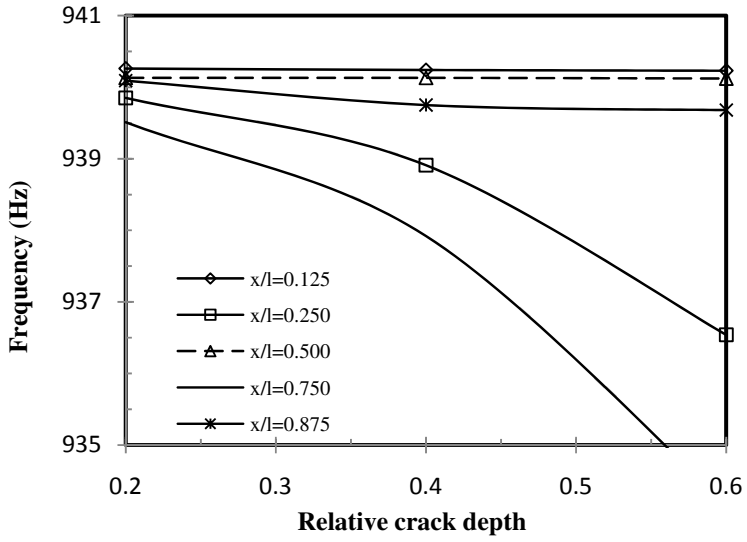

Fig. 6. Effect of relative crack depth on the 3rd frequency.

In Figs. 7-9 the influence of relative location of the crack on natural frequencies for different crack depths are investigated. Here, the relative crack length is fixed at 0.2. As shown in the figures, when the crack is placed at the plate modal nodes there is no change in natural frequencies of the plate. Moreover, the change in natural frequencies is in direct relation with the plate modal curvature. The maximum changes in natural frequencies take place when the cracks are located in the places with highest modal curvature.

Figs. 10-12 show the effect of crack length on the first three natural frequencies of the plate for a fixed crack depth. In these figures, the crack depth is fixed at 0.2.

The figures show that the crack length increase results in reduction in plate stiffness, and therefore a decrease in natural frequencies.

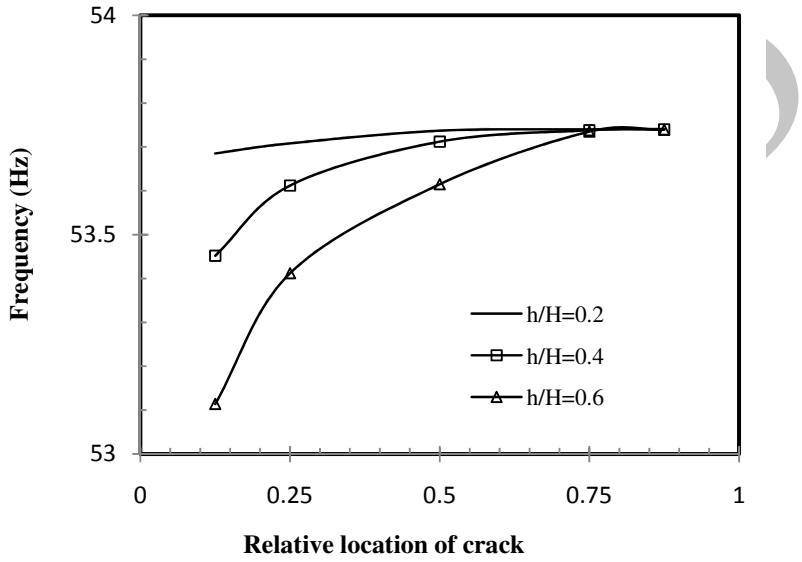

Fig. 7. Effect of relative crack location on the 1st frequency.

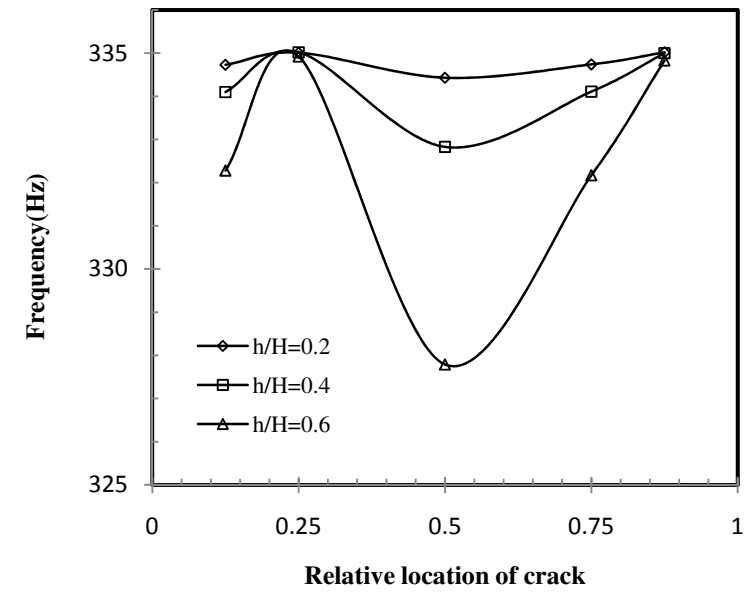

Fig. 8. Effect of relative crack location on the 2nd frequency.

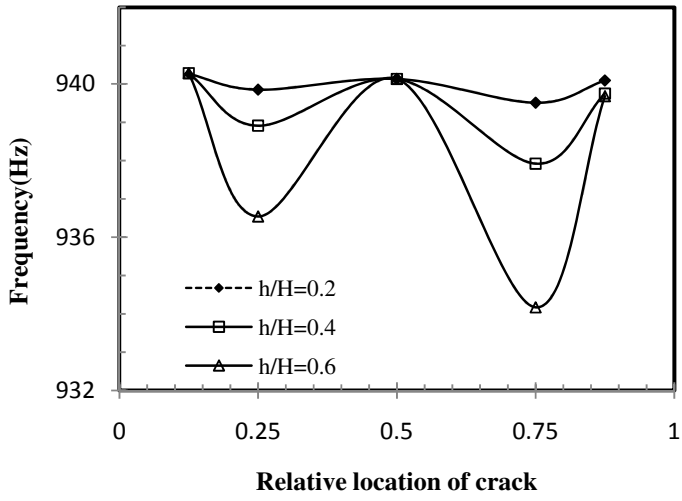

Fig. 9. Effect of relative crack location on the 3rd frequency.

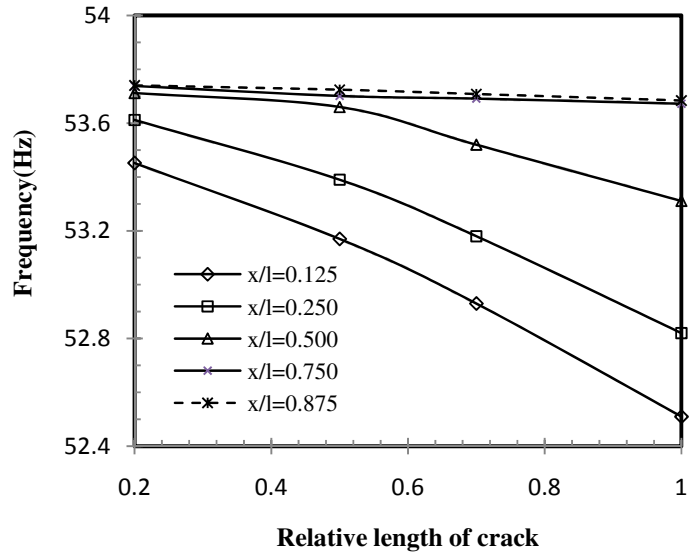

Fig. 10. Variation of 1st frequency due to increasing relative length of crack.

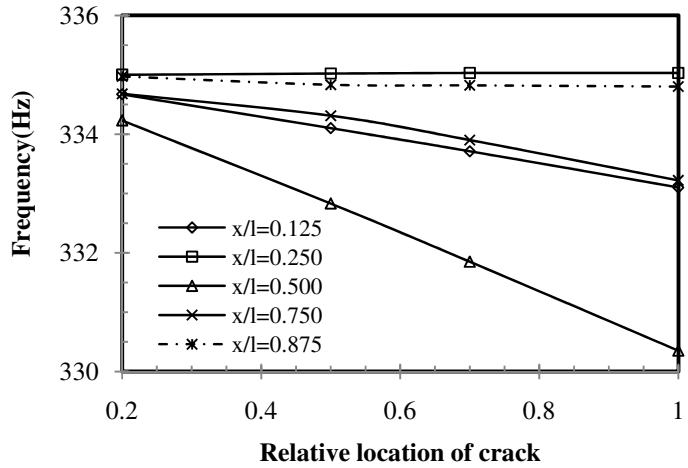

Fig. 11. Variation of 2nd frequency due to increasing relative length of crack.

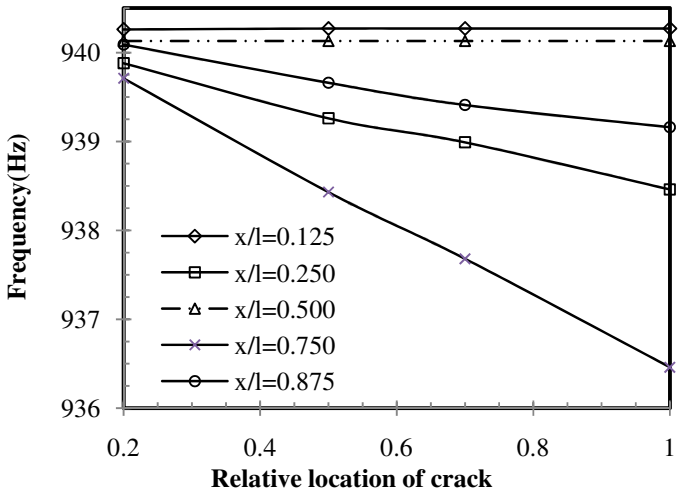

Fig. 12. Variation of 3rd frequency due to increasing relative length of crack.

4. Conclusions

The vibration behavior of cracked plates was investigated using differential quadrature method and experimental modal analysis. The crack was modeled using the well-known extended rotational spring model. The crack divided the plate into six segments. Then, the differential quadrature repre-senttation of governing differential equations of motion for each region along with the corres-ponding boundary and continuity conditions were formulated to obtain the natural frequencies of the cracked plate. Several experimental case studies on the cracked cantilever plates were conducted to ensure the integrity of the DQ method. Moreover, the influences of depth, location and length of crack on natural frequencies of the plate were studied. The results validate the applicability of the method for solving such an engineering problem. The method provides accurate results with rela-tively minimal computational and modeling efforts. It is concluded that the demon-strated accuracy and simplicity of the proposed method makes it a good candidate for modeling more complicated cases of cracked structures**.**

Reference

[1] Prabhakara, D.L.; Datta, P.K., "Vibration and Static Stability Characteristics of Rectangular Plates with a Localized Flaw", Journal of Computer and Structures, 1993,49, 5, pp. 825-836.

[2] Khadem, S.E.; Rezaee, M., "An Analytical Approach for Obtaining the Location and Depth of All-Over Part-Through Crack on Externally in-Plane Loaded Rectangular Plate Using Vibration Analysis", Journal of Sound and Vibration, 2000, 230, 2, pp. 291-308.

[3] Liew, K.M.; Hung, K.C.; Lim, M.K, "A solution method for analysis of cracked plates under vibration", Engineering Fracture Mechanics, 1994, 48, pp. 393-404.

[4] Ismail, R.; Cartmell, M.P., "An investigation into the vibration analysis of a plate with a surface crack of variable angular orientation", Journal of Sound and Vibration, 2012, 331, pp. 2929-2948.

[5] Xing, Y.; Liu, B., "Characteristic equations and closed-form solutions for free vibrations of rectangular Mindlin plates", Acta Mechanica Solida Sinica, 2009, 22, pp. 125-136.

[6] Fan, W.; Qiao, P., "A 2-D Continuous Wavelet Transform Of Node Shape Data For Damage Detection Of Plate Structures", International Journal of Solids and Structures, 2009, 49, pp. 4379-4395.

[7] Natarajan, S.: Baiz, P.M.; Ganapathi, M.; Kerfrien, P.; Bordas, S., "Linear free flexural vibration of cracked functionally graded plates in thermal

environment", Computers & Structures, 2011, 89, pp. 1535-1546.

[8] Hu, H; Wu, C., "Development Of Scanning Damage Index For The Damage Detection Of Plate Structures Using Modal Strain Energy Method", Mechanical Systems and Signal Processing, 2009, 23, pp. 274-287.

[9] Hosseini-Hashemi, S.; Roohi, H.; Rookni, H., "Exact Free Vibration Study of Rectangular Mindlin Plates with All-Over Part Through Open Cracks", Computers and Structures, 2010, 81, 4, pp. 329-345.

[10] Shahban, M.; Alipour, M.M., "Semi-analytical solution for free vibration of thick functionally graded plates rested on elastic foundation with elastically restrained edge" ", Acta Mechanica Solida Sinica, 2011, 24, pp. 340-354.

[11] Huang, C.S.; Leissa, A.W.; Li, R.S., "Accurate vibration analysis of thick, cracked rectangular plates", Journal of Sound and Vibration, 2012, 330, pp. 2079-2093.

[12] Huang, CS.; McGee III, O.G.; Chang, M.J., "Vibrations of cracked rectangular FGM thick plates", Composite Structures, 2011, 93, pp. 1747-1764.

[13] Rao, S.S., 2007, Vibration Of Continuous Systems, 1st ed., Hoboken, John-Wiley & Sons, Inc.

[14] Gross, B.; Srawely, J. E., "Stress-Intensity Factor for Single Edge Notch Specimens in Bending or Combined Bending and Tension by Boundary Collocation of Stress Function", NASA Technical Note,1965.